Roboustness of Hydrogen Bonding in the Construction of Supramolecular Architechures in Protonated Perchlorate Salts

D. Sathya
Anna University
N. Karthikeyan (karthin10@gmail.com)
Anna University https://orcid.org/0000-0001-8483-1378
R. Padmavathy
Quiad-E millath college for women
R. Jagan
Anna University
K. Saminathan
Anna University
R. Akilan
Aksheyaa College of Arts and Science

Research Article

Keywords: Perchlorate salts, hydrogen bonding, supramolecular studies, DFT calculations, Hirshfeld surface.

Posted Date: December 16th, 2021

DOI: https://doi.org/10.21203/rs.3.rs-1117206/v1

Abstract

Five new multicomponent salts of perchloric acid with a series of substituted anilines and N-heterocyclic amines namely Diphenylaminium perchlorate (DPAPC) **(1)**, 2, 5-dichloroanilinium perchlorate (25DAP) hydrate **(2)**, 4-Methylanilinium perchlorate (4MAPC) **(3)**, 4-diamino-6-methyl-1, 3, 5-triazin-1-ium hydrogen perchlorate (24DAMTHP) **(4)** and 8-hydroxyquinolinium hydrogen perchlorate (8HQP) **(5)** were prepared and structurally characterized. The entire complexes were subjected to FTIR and elemental analysis. A vast family of intermolecular contacts N-H…O, O-H…O, N-H…N and C-H…O were observed, which are key ingredient in the generation of privileged supramolecular self-assemblies appeared as one-dimensional chain, two-dimensional ladder and helix. Cambridge structural Database (CSD) analysis of 52 hits revealed the perchloric acid display higher propensity of ladder architectures. Molecular stability of the complexes were studied by quantum chemical calculations using DFT/B3LYP method with 6-31G(d,p) basis set. Further their relative charge distributions were identified using molecular electrostatic potential map. The use of Hirshfeld surfaces in combination with fingerprint plots was visualized in order to study the closer contacts within the molecule. The relative contribution of whole percentage of interactions associated is highlighted.

1. Introduction

Supramolecular chemistry takes advantage in the prediction and manipulation of intermolecular forces such as strong and weak hydrogen bonds, halogen-halogen contacts, π…π interactions, van der Waals forces for the intention to crystal design and engineering.[1–2] In particular the understanding of hydrogen bonding formation between the ionic molecules is being a primary focus because of its oddness in the progression of supramolecular chemistry with desired physical and chemical properties.[3] The crystal skeletons mainly depends on the shape and size of the interacting molecules and the availability of the functional groups leads to diversity of hydrogen bonds results in rich hydrogen bonding systems with new architectures [4]. The occurrence of strong and weak hydrogen bonds such as O––H….O, N––H…O, N––H….N and C––H…O establishes specific repeated architectures [5]. In supramolecular synthesis, the synthons (either Homo or Hetero) are the most reliable repetitive structural units of hydrogen bonds exerting its control over the assembly of molecules in crystalline materials [6–7]. The evolution of specific approach were widely utilized to generate robust aggregates and packing motifs in order to achieve a successful design of functional crystal solids, thus supramolecular synthons bridges between crystal engineering and organic synthesis [8–9].

Hybrid Organic-Inorganic structures are most promising composition since we can achieve new properties with desired features and functions [10]. Inorganic oxy-anions being very good donors and acceptors of special interest in forming strong intermolecular hydrogen bonds between cations and anions, showing innovative assemblies [11–12]. These anions act as templates or participate directly to crystal assembly as building units [13]. Among numerous oxy-acids, perchloric acid is considered to be one of the strong monobasic acids having certain unique properties that enable it where other strong acids fail. The negatively charged perchlorate ion is composed of one chlorine atom surrounded by four oxygen atoms arranged in tetrahedral geometry act as acceptor center to various hydrogen bond donors [14].

In structural consequences the peculiar habit of perchlorates are their self construction of ladder type architectures, which were archived from Cambridge Structural Database (version 5.35, May CSD 2015 release)

[17]. Similarly, In the crystal structure of guanidinium perchlorate, the anions and cations are self-assembled through hydrogen bonds constructing a two dimensional honey-comb type supramolecular framework [18]. On the other hand, Ammonium perchlorate can be regarded as the most important perchlorate salt used as an oxidizer in the composite solid propellants [19].

Huge number of systematic studies has been performed so far to achieve analogous type of architectures which are considered as the main framework in the Organic-Inorganic global crystal packing considerations. In connection with this, a sequence of five pechlorate salts (Figure 1) with substituted aromatic and N-Heterocyclic amines was prepared. Their structural phenomena in the context of supramolecular entity rendered due to the intermolecular hydrogen bondings in the crystal scaffolds were discussed. Additionally we intend to emphasis the closer molecular contacts via Hirshfeld surface analysis and associated two-dimensonal fingerprint plots.

2. Experimental Section

2.1. Diphenylaminium perchlorate (DPAPC) (1)

Diphenylaminium perchlorate (DPAPC) was prepared by taking equimolar amounts of diphenylamine 0.166g (1mM) and perchloric acid (0.06ml, 1mM) in methanol solvent. To the prepared methanolic solution of diphenylamine, diluted perchloric acid was added drop by drop followed by constant stirring at 40ºC. Stirring was continued for 30 minutes. The resultant mixture was kept free from atmospheric and physical disturbances for slow evaporation. Good diffraction quality crystals were obtained after four days. Anal. Calcd for C12H12ClNO4 (MW 269.68): C, 53.44; H, 4.49; N, 5.19. Found: C, 53.22; H, 4.39; N, 5.14 .The presence of functional groups was identified from the following FT-IR data (KBr, cm-1: 3332 (N-H), 3223 (C-H), 1553 (N-H), 1423(C-C), 1135 (C-N), 840 (O-Cl).

2.2. 2, 5-dichloroanilinium perchlorate (25DAP) hydrate (2)

Single crystals of 2, 5-dichloroanilinium perchlorate (25DAP) hydrate was prepared by taking equimolar amounts of 2, 5-dichloroaniline (0.164g, 1mM) and perchloric acid (0.06ml, 1mM) in methanol solvent. To the prepared methanolic solution of 2, 5-dichloroaniline, diluted perchloric acid was added drop by drop followed by constant stirring at 40ºC. Stirring was continued for 30 minutes. The resultant mixture was kept free from atmospheric and physical disturbances for slow evaporation. Good diffraction quality crystals were obtained after 3 weeks. Anal. Calcd for C6H8Cl3NO5 (MW 280.48): C, 25.69; H, 2.87; N, 4.99. Found: C, 25.62; H, 2.65; N, 4.84.The presence of functional groups was identified from the following FT-IR data (KBr, cm-1): 3562 (O-H), 2783(N-H), 2553(C-H), 1513(N-H), 1133(C-N), 830 (O-Cl).

2.3. 4-Methylanilinium perchlorate (4MAPC) (3)

4-Methylanilinium perchlorate (4MAPC) was prepared by taking equimolar amounts of 4-methylaniline (0.107g 1mM) and perchloric acid (0.06ml, 1mM) in methanol solvent. To the prepared methanolic solution of 4-methylaniline, diluted perchloric acid was added drop by drop followed by constant stirring at 40ºC. Stirring was continued for 30 minutes. The resultant solution was allowed to evaporate slowly at ambient conditions. Good colourless diffraction quality crystals were formed after seven days. Anal. Calcd for C7H10ClNO4 (MW

207.61): C, 40.50; H, 4.85; N, 6.75. Found: C, 46.55; H, 7.06; N, 21.63. The presence of functional groups was identified from the following FT-IR data (KBr, cm-1): 2982 (O-H), 2814 (N-H Stretch), 1693 (C-H), 1594 (C-C), 1543 (N-H), 1133 (C-N), 893 (O-Cl).

2.4. 2, 4-diamino-6-methyl-1, 3, 5-triazin-1-ium hydrogen perchlorate (24DAMTHP) (4)

24DAMTHP was prepared by taking equimolar amounts of 2, 4-diamino-6-methyl-1, 3, 5-triazine (0.166g (1mM)) and perchloric acid (0.06ml, 1mM) in methanol solvent. To the prepared methanolic solution of 2, 4-diamino-6-methyl-1, 3, 5-triazine, diluted perchloric acid was added drop by drop followed by constant stirring at 40ºC. Stirring was continued for 30 minutes. The resultant mixture was kept free from atmospheric and physical disturbances for slow evaporation. Good diffraction quality crystals were obtained after one week. Anal. Calcd for C4H8ClN5O4 (MW 225.59): C, 21.30; H, 3.57; N, 31.4. Found: C, 21.25; H, 3.48; N, 31.4. The presence of functional groups was identified from the following FT-IR data (KBr, cm-1): 3393 (O-H), 3022 (broad) (N-H), 1753 (C-H), 1693(C-C), 1133(C-N).

2.5. 8-hydroxyquinolinium hydrogen perchlorate (8HQP) (5)

8-hydroxyquinolinium hydrogen perchlorate (8HQP) was synthesized from the 1:1 mixture of 8-hydroxyquinoline (0.14g 1mM) and perchloric acid (0.06ml 1mM). To the prepared methanolic solution containing 8-hydroxyquinoline a solution of HClO4 diluted with methanol was added slowly drop wise. The resulting solution was stirred for 30 minutes with constant heating at 40°C and then the mixture was allowed to stand at room temperature for slow evaporation. After two weeks suitable crystals for diffraction studies were collected. Anal. Calcd for C9H8ClNO5 (MW 245.62): C, 44.01; H, 3.28; N, 5.70. Found: C, 43.95; H, 3.14; N, 5.63. The presence of functional groups was identified from the following FT-IR data (KBr, cm-1) 3822 (O-H), 3173(N-H), 2262 (C-H), 1684 (C-C), 1663 (C-C), 1383(C-N), 850 (O-Cl).

3. Results And Discussion

All the compounds were characterized by Single crystal X-ray diffraction method in order determine their crystal structure, supramolecular organization and theoretical calculations were done to explore their molecular stability and dense intermolecular interactions.

3.1. X-ray crystallography

The structure refinement parameters of compounds 1 to 5 are given in Table 1. The geometrical characteristics of hydrogen bonds are given in Table 2. Intensity data for all the crystals were collected using a Bruker AXS Kappa APEX II single crystal CCD diffractometer equipped with graphite-monochromated MoKα radiation at room temperature. Accurate unit cell parameters were determined using reflections collected from 36 frames measured in three different crystallographic zones and using the method of difference vectors. All the crystal structures were solved by conventional direct methods procedure using SHELXS-97 program. The positions of all the non-hydrogen atoms were included in the full-matrix least squares refinement using SHELXL97 program [20]. Normalized structure factors were used for finding the phases. The positions of all the hydrogen atoms were identified from difference electron density peaks, and they were constrained to ride

on the corresponding non-hydrogen atoms. The hydrogen atom bound to carbon atoms are constrained to a distance of C-H = 0.93 - 0.97Å and Uiso(H) = 1.2Ueq(C) and 1.5Ueq(C). The hydrogen atom associated with the nitrogen atom was identified from the difference electron density maps and were subsequently fixed on the same position with a distance of d(N-H) = 0.89Å and Uiso(H) = 1.5Ueq(N).

Table 1
Crystal Structure and Refinement Parameters of compounds 1-5

Parameters	1	2	3	4	5
Moiety Formula	$C_{12}H_{12}N^{+}.ClO_4^{-}$	$C_6H_6Cl_2N^{+}.ClO_4^{-}$	$C7\ H_{10}\ N^{+}.ClO_4^{-}$	$C_4H_8N_5$+ $.ClO_4^{-}$	$C_9H_8NO_2^{+}.ClO_4^{-}$
Empirical formula	$C_{12}H_{12}ClNO_4$	$C_6H_6Cl_3NO_4$	$C_7H_{10}ClNO_4$	$C_4H_8ClN_5O_4$	$C_9H_8ClNO_4$
Formula weight	269.68	280.48	207.61	225.60	245.61
Temperature(K)	293(2)	293(2)	293(2)	293(2)	293(2)
Wavelength(Å)	0.71073	0.71073	0.71073	0.71073	0.71073
Crystal system, space group	Triclinic, P-1	Triclinic, P-1	Monoclinic, P21/c	Triclinic, P-1	Monoclinic, $P2_1/n$
Unit cell dimensions					
a(Å)	9.4559(6)	a = 7.3709(3)	9.5217(12)	a = 7.0640(3)	a = 8.5008(7)
b(Å)	9.9909(6)	b = 7.5218(3)	7.2062(7)	b = 8.3325(3)	b = 5.4932(4)
c(Å)	14.7973(9)	c = 10.7559(5)	14.3140(18)	c = 8.6039(3)	c = 22.0567(18)
α(º)	93.263(3)	76.2210(10)	90	64.254(2)	90
β(º)	94.047(3)	79.426(2)	90.109(4)	83.251(2)	98.752(2)
γ(º)	114.094(3)	67.5290(10)	90	85.051(2)	90
Volume $Å^3$	1267.31(13)	532.35(4)	982.2(2)	452.65(3)	1017.98(14)
Molecules/Unit cell, Z	4	2	4	2	4
Calculated density Mg/m^3	1.413	1.750	1.404	1.655	1.603
Absorption coefficient mm^{-1}	0.307	0.860	0.372	0.423	0.381
F(000)	560	284	432	232	504
Crystal size mm	0.30 x 0.25 x 0.20	0.35 x 0.30 x 0.25	0.25 x 0.20 x 0.20	0.35 x 0.30 x 0.25	0.30 x 0.30 x 0.25
θ range for data collection (º)	1.39 to 27.50	1.96 to 27.50	1.42 to 28.97	2.64 to 26.00	2.46 to 26.00

Parameters	1	2	3	4	5
Limiting indices	-12<=h<=12, -12<=k<=12, -19<=l<=19	-9<=h<=9 -9<=k<=9 -13<=l<=13	-12<=h<=12, -5<=k<=9, -19<=l<=19	-8<=h<=8 -10<=k<=10 -10<=l<=10	-10<=h<=10 -4<=k<=6 -27<=l<=25
Reflections collected / unique	28209 / 5808	15705 / 2441	12641 / 2605	8417 / 1772	10556 / 2001
R(int) / R(sigma)	0.0316	0.0325	0.0342	0.0262	0.0293
Completeness to θ = 28.51 (%)	99.80%	99.9%	99.90%	99.6%	99.9%
Max. and Min. transmission	0.9411 and 0.9135	0.9192 and 0.8414	0.9292 and 0.8627	0.9017 and 0.8661	0.9109 and 0.8944
Data / restraints / parameters	5808 / 0 / 325	2441 / 5 / 160	2605 / 0 / 122	1772 / 4 / 149	2001 / 0 / 158
Goodness-of-fit on F^2	1.169	1.061	1.017	1.063	1.052
Final R indices [I>2sigma(I)]	R1 = 0.0540, wR2 = 0.1636	R1 = 0.0399, wR2 = 0.1101	R1 = 0.0528, wR2 = 0.1496	R1 = 0.0519, wR2 = 0.1502	R1 = 0.0333, wR2 = 0.0899
R indices (all data)	R1 = 0.0747, wR2 = 0.1790	R1 = 0.0423, wR2 = 0.1128	R1 = 0.0825, wR2 = 0.1720	R1 = 0.0544, wR2 = 0.1528	R1 = 0.0386, wR2 = 0.0957
Largest diff. peak and hole e.A^{-3}	0.489 and -0.401	0.619 and -0.460	0.352 and -0.235	0.770 and -0.565	0.277 and -0.318

Table 2
Geometrical parameters for hydrogen bonds in compounds 1-5

COMPOUND	A	H	B	A-H	H…B	A…B (Å)	A-H…B (°)	symmetry operation
1	N1A	H1A2	O3A	0.9	1.96	2.839(3)	166.5	-x+1,-y+2,-z+1
	N1B	H1B1	O4B	0.9	1.9	2.796(3)	176.5	-x+1,-y+1,-z
	N1A	H1A1	O2A	0.9	2.14	2.995(4)	159.6	----
	N1B	H1B2	O1B	0.9	1.99	2.886(3)	175.1	----
	C2B	H2B	O1A	0.93	2.57	3.316(4)	137.2	-x+1,-y+1,-z+1
	C1A	H1A	O4A	0.93	2.48	3.214(4)	135.6	x-1,y,z
2	O1W	H1W	O1	0.903(10)	2.196(18)	3.050(3)	158(4)	----
	O1W	H2W	O3	0.914(10)	2.15(2)	3.014(3)	158(5)	x,y+1,z
	N1	H1C	O1	0.885(10)	1.931(11)	2.808(3)	170(3)	x+1,y-1,z
	N1	H1B	O2	0.882(10)	2.066(14)	2.923(3)	164(3)	-x+1,-y+1,-z
	N1	H1B	O4	0.882(10)	2.52(3)	2.951(3)	111(3)	x+1,y,z.
	N1	H1A	O1W	0.888(10)	2.30(3)	2.923(3)	127(3)	-x+1,-y+1,-z
	N1	H1A	O3	0.888(10)	2.21(2)	2.991(3)	146(3)	-----
3	N1	H1A	O4	0.89	2.24	2.865(5)	126.8	-x,y+1/2,z+1/2
	N1	H1A	O3	0.89	2.3	2.937(4)	128.1	x,y+1,z
	N1	H1C	O1	0.89	2.04	2.899(5)	160.5	-x,-y+1,-z
	N1	H1B	O4	0.89	2.29	3.166(4)	168.8	---
4	N5	H5A	N2	0.89	2.158(12)	3.042(3)	172(3)	-x+2,-y+2,-z
	N5	H5B	O1	0.89	2.30(2)	3.091(4)	148(3)	x+1, y,z-1
	N4	H4E	O3	0.89	2.13(2)	2.875(4)	141(3)	-x,-y+1,-z+1;
	N4	H4D	O2	0.89	2.12(2)	2.974(4)	159(5)	x,y,z-1.
	N1	H1A	O4	0.79	2.05(4)	2.826(3)	172(3)	----
5	O5	H7	O1	0.82	1.93	2.7438(18)	173.4	-x+3/2,y-1/2,-z+1/2
	N1	H1A	O1	0.83(2)	2.05(2)	2.864(2)	165(2)	----

3.1.1. Crystal structure of Diphenylaminium perchlorate (DPAPC) (1)

The crystal structure of DPAPC crystallizes in monoclinic system with P21/n space group with two set of anions and cations in the asymmetric unit. Both the diphenylaminium cations A and B in DPAPC experience certain steric effects. This has been revealed from the difference in the geometrical parameters of the protonated and the neutral diphenylamine molecule. The supramolecular organic-inorganic framework in DPAPC is primirarly decided by four N—H…O hydrogen bonds and two C—H…O interactions. The H atom of the perchloric acid transfer to one of the N atoms of the diphenylamine molecule. The A and B sets of molecular ions independently form supramolecular networks as discussed below. In molecule A, two N—H…O hydrogen bonds N1A—H1A1…O2A and N1A—H1A2…O3A connect the centrosymmetrically related HClO4- anions and diphenylaminium cations forming a $R_4^4(12)$ motif, with the centroid of the motif occupying the crystallographic inversion centre along (1/2, y, 1/2). A C—H…O interaction, C1A—H1A…O4A connects these centrosymmetrically related

$R_4^4(12)$ motif resulting in the formation of a $R_2^4(16)$ herterocyclic motif around the inversion centres along (0, y, 1/2). Both the $R_4^4(12)$ and $R_2^4(16)$ motifs fused to form an one dimensional supramolecular ladder extending along [1 0 0] direction. Similar type of ladder framework is also formed by the self-assembly of B molecular sets of ions. The anions and cations of B set of molecules are linked through the hydrogen bonds N1B—H1B2…O1B and N1B—H1B1…O4B forming a ring motif around the centre of inversions at (1/2, 0, z). These motifs are further bonded through the C2B—H2B...O1A forming a centrosymmetric $R_2^4(18)$ motif along (0, 1/2, z) by generating an infinite one dimensional supramolecular ladder along [1 0 0] direction and is depicted in Figure 2.

3.1.2. Crystal structure of 2, 5-dichloroanilinium perchlorate (25DAP) hydrate (2)

The asymmetric unit of 25DAP comprises one perchlorate anion, one 2, 5-dichloroanilinium cation and a water molecule. The salt 25DAP crystallizes in triclinic system with P-1 space group. The hydrogen bonded organic-inorganic supramolecular frameworks of 25DAP are determined primarily by combination of O-H…O and N-H…O hydrogen bonds. The perchlorate anion of four oxygens exhibit two O-H...O and three N-H...O hydrogen bonds, in which atom O3 act as a bifurcated acceptor with O1W and N1. The supramolecular frameworks of 25DAP stabilized by N-H…O and strong O-H…O hydrogen bonds through water molecule. The N1 atom of anilinium cation involves five N-H...O hydrogen bonds in a bifurcated fashion with oxygen atom of three anions and two water molecules. The ClO_4^- anion forms two N-H…O hydrogen bonds with amino N1-H1 and N1A-H1B group at the point of O2 and O3, which then leads to the formation of a 1D infinite chain along c axis. Adjacent chains are further connected by a N-H...O hydrogen bond between the amino NH (N1-H1B) group and O2 atom of perchlorate anion, leading to

formation of 1D molecular ladder contains centro-symmetrically related $R_4^4(12)$ and $R_2^4(8)$ graph-set motifs as shown in Figure. The water molecule plays an important role in the assembly of the solid-state structure and the multiple hydrogen bonding interactions around the water molecule are particularly interesting. The O1W atom of water molecule acts as both donor and acceptor and form a bifurcated N–H…O bonds. Further the ladders are bridged by water molecule through two O-H...O (O1W-H1W...O1 and O1W-H2W...O3) and N-H...O (N1-H1C...O1W and N1-H1A...O1W) hydrogen bonds forming two dimensional bilayer assembly. The symmetry related water molecule involves the intermolecular interactions to form a variety of ring motifs such as $R_4^2(8)$, $R_4^4(8)$ and $R_3^3(8)$ giving a self-assembled three dimensional net as shown in Figure 3.

3.1.3. Crystal structure of 4-Methylanilinium perchlorate (4MAPC) (3)

The asymmetric unit of 4MAPC comprises of one perchlorate anion and one

4-methylanilinium cation. The salt 4MAPC crystallizes in monoclinic space group P21/c. The basic supramolecular framework and the molecular packing between the molecular ions in 4MAPC are primarily decided by four N—H…O hydrogen bonds. In 4MAPC, salt the symmetry related anions and cation are linked through two N-H…O hydrogen bonds N1—H1A…O3 and N1-H1C…O1 to form a supramolecular motif $R_4^4(12)$ around the crystallographic centre of inversion along (0 0 z). The $R_4^4(12)$ ring motif positioned at the unit translation along [0 1 0] is further connected through a hydrogen bond N1—H1B…O4 form an additional supramolecular motif of the same type with N1-H1C…O1 hydrogen bond. The motif thus formed also occupies the crystallographic inversion center along (0, 1/2, z). The infinite translation of both the motifs construct a one dimensional ladder super-molecule along [0 1 0] direction and the same is illustrated in Figure. The 2_1 screw related adjacent ladders are linked through the hydrogen bond N1—H1A…O4 with the screw axis along (0, y, 1/4). These linkages construct a two dimensional sheet of anions and cations

built from repetitive motifs of $R_4^4(12)$ and $R_3^3(8)$ extending parallel to the (1 0 0) plane and is shown in Figure 4. The adjacent molecular (1 0 0) sheets are stacked by unit translation along c-axis.

3.1.4. Crystal structure of 2, 4-diamino-6-methyl-1, 3, 5-triazin-1-ium hydrogen perchlorate (24DAMTHP) (4)

The structure of 24DAMTP composed of one molecule of cation and one molecule of perchlorate anion in the asymmetric unit and the crystal crystallizes in triclinic system with P-1 space group. The basic supramolecular framework and the molecular packing between the molecular ions in 24DAMTP are primarily decided by four N—H…O and one N-H…N hydrogen bonds. Out of five nitrogens in cation, two amino nitrogens

involves three N-H…O hydrogen bonds and two hetero cyclic nitrogen exhibits one N-H…O and N-H…N interactions respectively. The heterocyclic N3 atom doesn't involve any other interactions. The trizinium cation are connected to perchlorate anion through a pair of three N-H…O hydrogen bonds N4-H4E…O3, N4-H4D…O2 and N1-H1A…O4 interactions

forms centrosymmetric ring motifs $R_4^4(16)$ and $R_4^4(12)$to generate one dimensional ladder running along [1 0 0] direction as depicted in Figure. Further the adjoining molecular ladders are interlinked through centrosymmetric $R_2^2(8)$ ring motif to create two dimensional sheet as depicted in Figure. Centrosymmteric coplanar triazinium cation forms a significant R22(8) ring motif through N5-H5A…N2 homo dimer, which is one of the most frequently occurring bimolecular cyclic hydrogen-bonded units in organic crystal structures [21]. The 2D sheet linked by N5-H5…O1 hydrogen bond to generate three

dimensional molecular net Figure 5. Additionally, the weak C-H…O interaction (C4-H4C…O2) observed between the methyl group of C atom with perchlorate anion to stabilizing the supramolecular architectures.

The organic-inorganic triazine compounds forms interesting supramolecular frameworks through manifold hydrogen bonds due to the presence of hydrogen bonding sites [22–23]. The heterocyclic system of 2, 4-diamino-6-methyl- 1, 3, 5-triazine comprises three ring nitrogen and two amino groups. Of the different sites available in the triazine molecule, protonation occurs at one of the ring N atom ortho to the C atom of methyl group. The protonation of N2 atom causes a redistribution of π-electron density so that the resulting distortions in the molecular geometry of the cation suggest that the charge-separated two type quininoid forms are significant contributors to the overall molecular structure [24–25]. In 24DAMTP, the perchlorate anion of four oxygen atoms involves intermolecular interactions with the donor atoms forming a distorted tetrahedral arrangement. This type of arrangement is less common than a three-coordinated one, with the Cl atom on top of a more or less flattened tripodal coordination pyramid [26].

3.1.5. Crystal structure of 8-hydroxyquinolinium hydrogen perchlorate (8HQP) (5)

In 8HQP consists of the perchlorate anion and 8-hydroxy quinolinium cation in the asymmetric unit. Compound 8HQP crystallizes in monoclinic system with spacegroup P21/n. The interaction between the ions are stabilized by strong N—H…O,

O-H…O and weak C—H…O interactions. In 8HQP, the bifunctional hydrogen bonding 8-hydroxyquinolinium cation in protic solvents simultaneously acts as an H donor at the O-H group and as an H acceptor at the N atom. The N-H…O and O-H…O intermolecular interactions plays major role in the construction the supramolecular frameworks. The perchlorate anion connected with 8-hydroxyquinolinium cation via N1-H1A…O2 and O5-H7…O2 hydrogen bonds generates one dimensional helical structure along [1 0 0] direction Figure 6. The anionic oxygen atom O2 of chain extends its contribution to the supramolecular self-organization by acting as bifurcated hydrogen bonded acceptor to the hydroxyl (O––H) and amino (N+––H) centers of the cations. The C-H group of cations contributes to C1––H1….O3 (C…O = 3.348 Á) and C3––H3….O1 (C…O =

3.452 Å) hydrogen bond interactions between the helical chain builds up a three dimensional molecular network.

The involvement of HClO4 in specific ladder type super-molecule construct is observed in all the compounds with the aid of strong N-H…O interactions except in 8-hydroxyquinolinium perchlorate, while it forms 2D helical architecture and it may be due to the presence of hydroxyl group closer to the acceptor site.. The presence of water molecules in compound (2) leads to the formation of additional O-H…O hydrogen bonds in the architecture, results in higher hierarchy assemblies.

A huge number of compounds with perchlorate anion have been deposited in CSD V5.35. The structures with disorders, solvents, inorganic complexes were filtered and the structures relevant for the present analysis were considered. Perchlorate anions with cations form a variety of architectures with cations and other molecules. From the list of structures archived from CSD the structures AVOQOD, HIRMOL, JUQCON, PEMMEA, PIXMOZ, ROGCUM and WENAP form ladder type supramolecular architectures with R44(12) and R42(8) which extends further to higher dimensional networks. In the structures AVOQOD, JUQCON, PEMMEA, PIXMOZ and ROGCUM, the molecular

ladders are built from repeated motifs of $R_4^4(12)$ whereas in HIRMOL and ROGCUM the molecular ladders are built from alternate motifs of $R_4^4(12)$ and$R_2^4(8)$. It is of interest to note that the cationic molecule involved in these supramolecular constructions of ladders are aniline and substituted anilines. As observed in the compound 2, the crystal structure of 2-aminophenylaminium perchlorate hydrate [35] (Raghavaiah et al 2005) the anions and cations form $R_4^4(12)$ motif which is further bridged by water molecules to form a supramolecular ladder. From the above discussions, the supramolecular similarity in the perchlorate salts shows the selection of anilinium cation can form ladder type architecture consisting of $R_4^4(12)$ and $R_2^4(8)$. Variety of supramolecular synthons present in perchlorate salts 1-5 were given in Figure 7.

3.2. Hirshfeld Surface Analysis

Nowadays a great deal of attention has been paid to Hirshfeld surface (HS) analysis due to its peculiarity in direct visualization of dense intermolecular contacts in colored mapping [27]. Such important prediction makes ease understanding of how molecule interacts within its molecular environment, provides a significant understanding to communicate the structure to its properties. [28]. While the supramolecular approach lacks in clarifying such fundamental chemical interactions governing even the simplest self-assembly processes to obtain atomic-level information [29]. On the other hand two dimensional fingerprint (FP's) plots represent major advances in enabling quantitative insight into the whole molecular interactions associated within the molecular crystal [30]. The quantities d_e and d_i are the distance characterized from hirshfeld surface to outside and inside atoms respectively where the measure d_{norm} is the normalized contact distance between them, displays the surface in three distinguishable colored contours representing bright red spots as shorter contacts, white areas as contacts closer to van der Waals separation and blue regions as close contacts.

The hirshfeld surface analysis and associated 2D fingerprint plots were analyzed for the compounds 1-5 over the d_{norm} range of - 0.5 to 1.4 Å are illustrated in Figures 6-10 using Crystal Explorer program [31]. The hirshfeld surfaces were mapped for cation sites in all the compounds (Figure 8-12) in order to facilitate its reactivity with anionic counterpart. The surfaces were also presented as transparent to clarify their structural diversity with the neighboring atoms.

From the hirshfeld surfaces it was clearly observed that all the five salts shows dominant H…O interaction engaged in the short N-H…O hydrogen bonding between the perchlorate anion with adjacent cations appeared as bright red over the surface. Consequently a similar H…O contacts was also found in compound 2 between the two hydrogen atoms of the water molecule with the closest oxygen of oxyanions resulting in the formation of strong O-H…O interaction, while in the case of 5 the similar interactions was traced among oxygen atoms of anionic moiety to the neighboring hydroxyl group. It is noteworthy that a homo dimeric synthon was naturally occurred between triazine derivatives via amine (NH_2) and the heterocyclic nitrogen's bridged through N-H…N hydrogen bonding depicted as dark red regions on the hirshfeld surface. Interestingly a weak C-H…O interactions was also observed in all the compounds as H…O contact due to the interconnection between the aromatic CH of the cations with the nearest anionic oxygen's found as light red spots in the surface.

Two dimensional fingerprint plots were drawn to explore the percentage of intermolecular interactions involved in the compounds shown in Figure 6 - 10. As expected the dominant nature of H…O contact appeared as sharp spikes for all the compounds, most of the region in the plot is occupied by this contact due to the N-H…O, C-H…O and O-H…O hydrogen bonds facilitate in the construction of unusual supramolecular self assemblies. The anticipated propensities of H…O contacts are 33.2% in **1**, 26.7% in **2**, 39.8% in **3**, 36.4% in **4** and 39.7% in **5**. The notable proportion of π…H and H…π contact are found as lower and upper spikes is related to the characteristic C…H and H…C interaction exist between the phenyl ring with the adjacent molecules in all the compounds excluding 4. Moreover a large variance of H…H interaction is noted for the above salts which represent the contacts between the aromatic and amino hydrogens in the aryl unit of cations with their symmetrical neighbors. Interestingly the Cl…H contact was found in compound 2 arise due to the C-H…Cl interaction between the substituted chlorine atom of aniline with the surrounding aromatic protons (CH). Similarly the meta Cl atom interacts with the oxygen atoms of inorganic anion are given through Cl…O contact. In the case of 4, the strong N-H…N interaction plays a vital role in the existence of homo dimer are viable through H…N and N…H interactions shown as upper and lower sharp spikes. Further a small proportion of C…O contact was pointed in compound 5 due to lone pair…π interaction between the counter ions. The relative contribution of overall interactions involved in all the five salts was clearly as depicted as Histogram in Figures 8 – 12. Thus the above study on whole summarizes the crystal structure of molecules have prominent signatures due to hydrogen bonding which plays major role in the assembly of fascinating three dimensional supramolecular entities.

3.3. Theoretical Calculations

To support the experimentally determined molecular structure the compounds were geometrically optimized under DFT calculations. In this study the quantum chemical calculation were performed using Gaussian 09W [32] software using 6-31G(d,p) basis set at DFT/B3LYP theory [33–34]. The structures were minimized to global energy minima -1191.7821 a.u. **(1)**, -1238.4988 a.u. **(2)**, -2044.5525 a.u. **(3)**, -1088.2655 a.u. **(4)** and

-2559.9626 a.u. **(5)**. Good agreement was achieved between the calculated and crystal geometry. On keen observation the differences in the values of 0.03(7) Á and 0.04(9) Á for C-C bond, 0.4(3) Á and 0.3(3) Á for N-C bond, 3.3(0)^{o} and 3.4(9)^{o} for O-C-C bond angle respectively. Figure 14 shows the optimized molecular structures of the compounds 1-5. The discrepancies found may be change in phase of the system where the experimental structure belongs to crystalline state where intermolecular interactions play a major role while the predicted geometry is at gas state. No constraints and restraints were involved the molecules were allowed free to optimize.

In correlation with above the molecular electrostatic potential mapping was carried out in order to visualize the relative charge distribution within the molecules as ancillary tool using theoretical calculations [35]. For a better comparison of MEP's the electron density isovalues and the colors for the contouring were kept symmetrical as shown in Figure 13. Generally the green regions found in molecular electrostatic potential maps are due to neutral charges on the surface which is very close to zero. In all salts the electron clouds (red and yellow regions) are localized around oxygen atoms of oxyanions indicates the negative electrostatic potential mainly due to electrophillic reactivity. Accordingly the nucleophillic sites (blue regions) are accumulated around the protons of amine group in the cation. Hence this study also evident the molecular structure of the salts are hardly dominated by N-H…O strong hydrogen bonding as explained in X-ray diffraction study and hirshfeld surface analysis.

4. Conclusion:

In summary, we have demonstrated the structural stragedy of five perchlorate salts with substituted aniline and N-heterocyclic amines. Interplay of strong N-H…O, O-H…O, N-H…N and weak C-H…O hydrogen bondings were characterized. The use of expected intermolecular contacts framed by regular $R_4^4(12)$ and $R_2^4(8)$ ring motifs provide wide range of supromolecular synthons. The robustness of homo and hetero sythons was established in the construction of fascinated ladder and helical type supramolecular architectures. Structures retrieved from CSD feature the similar ladder assemblies in supramolecular building blocks in terms of perchlorate moiety as good hydrogen donor. Theoretical calculations were performed at ground state using DFT method, the optimized geometries shows good agreement with crystal structure. Hirshfeld surface analysis of all compounds 1-5 shows the existence of N-H…O, O-H…O, N-H…N and C-H…O parallel contacts which involved in the stabilization of the crystals. Interpretation of two dimensional fingerprint plots show existence of characteristic H…O, H…H, C…H, N…H and other short contacts piled up in the molecular structure. Overall the study discuss the perchlorate oxyanion denotes in the forecasting of one, two and three dimensional periodic superstructures.

Declarations

Authors' contributions:

Experimental work, data interpretation and article writing: D. Sathya, N. Karthikeyan, R. Padmavathy; Editing and discussion: R. Jagan and K. Saminathan; Final review: R. Akilan.

Funding: Not Applicable

Availability of data and material:

Crystallographic data of the structure reported in this article have been deposited in the Cambridge Crystallographic data centre. The deposition numbers are CCDC- 1409707-1409711. Copy of the data can be downloaded at free charge from CCDC website (www.ccdc.cam.ac.uk). Experimental and Theoretical bond length and angles were tabulated in Supplementary article.

Code availability:

The calculations were performed using Gaussian 09 W and GaussView 5.0 and Hirshfeld surface analysis were done using Crystal Explorer.

Ethics approval: Not applicable

Consent to participate : Not applicable

Consent for publication: Yes

Conflicts of interest: The authors declare no competing interests.

Acknowledgements

The authors thank SAIF, IIT Madras for the Single crystal X-ray diffraction facility.

References

1. C. B. Aakeroy and A. M. Beatty, Aust. J.Chem., 2001, 54, 409–421.

2. G.R. Desiraju, Crystal Engineering: The Design of Organic Solids, Elsevier, Amsterdam, 1989.

3. (a) Zhang, J.; Wu,L.; Fan, Y.; J.Mol.Struct., 2003, 660, 119 (b) S. Jin.; Liu, L.; Wang, D. Guo, J.; J. Mol.Struct., 2011, 1005, 59. (c) Ballabh, A.; Trivedi, D.R.; Dastidar, P.; Suresh, E.; Cryst.Eng.Comm., 2002, 4, 1135.

4. (a) Sethuraman, V.; Stanley, N.; Thomas Muthiah, P.; Sheldrick, W. S.; Winter, M.; Luger.P; Weber, M. Cryst.Growth Des., 2003, 3, 823. (b) Miao Du.; Zhi-Hui Zhang.; Xiao-Jun Zhao.; Hua Cai.; Cryst. Growth Des., 2006, 6, 1186. (c) Krishnamohan Sharma, C. V.; Cryst Growth Des., 2002, 2, 465.

5. (a) Allen, F.H.; New. J.Chem., 1999,25. (b) Zi-Liang,W.; Lin- Heng, W.; Lin-Yu, J.; Jing Ping, W.; Chinese J. Struct. Chem., 2007, 26, 12, 1423. (c) Thakuria, H.; Borah, B. M.; Pramanik, A.; Das, G. J.Chem.Crystallogr., 2007, 37,807.

6. D.Shekhar Reddy, Yuri E. Ovchinnikov, Oleg V. Shishkin,Yuri T. Struchkov and Gautam R. Desiraju, J. Am. Chem. society, 1996, 118, 4085.

7. V. Sethuraman, N. Stanley, P. Thomas Muthiah,W. S. Sheldrick, M. Winter, P. Luger and M. Weber, Crystal growth and design, 2003, 3, 823.

8. F. H. Allen, W. D. S. Motherwell, P.R. Raithby, G. P. Shieldsa, and R. Taylora, New J. Chem., 1999, 25-34.

9. Man Shing Wong, Volker Gramlich, Christian Bosshard and Peter Gu¨nter, J. Mater. Chem., 1997, 7(10), 2021–2026.

10. P. Judeinstein and C. Sanchez, J. Mater. Chem., 1996, 6, 511-525

11. A. Abate, J. Martí-Rujas, P. Metrangolo, T. Pilati, G. Resnati , and G. Terraneo, Cryst. Growth Des., 2011, 11 (9), 4220–4226.

12. T. Diop, L. Diop, C. A. K. Diop, K. C. Molloy and G. Kociok-Köhn, Acta Cryst., 2011, E67, m1872 - m1873.

13. R. Custelcean, Chem. Soc. Rev., 2010, 39, 3675–3685.

14. G. M. Brown and B. Gu. Perchlorate, Springer, 2006, pp 17-47.

15. F. H. Allen. Acta Cryst. 2002, B58, 380–388.

16. M. Szafranski. J. Phys. Chem., 2011, 115, 8755–8762.

17. S. Vyazovkin and C. A. Wigh, Chem. Mater. 1999, 11, 3386-3393.

18. M. Drozd. And D. Dudzic. Spectrochim. Acta A. 2013, 113, 345–356.

19. S. Vyazovkin and C. A. Wigh, Chem. Mater. 1999, 11, 3386-3393.

20. G. M. Sheldrick, . “A short history of SHELX”, Acta Cryst, 2008, A64, 112-122.

21. T. Steiner. Angew. Chem. Int. Ed. 2002, 41, 48-76.

22. John C. MacDonald , George M. Whitesides, Chem. Rev., 1994, 94 (8), 2383–2420.

23 . Jan Janczaka and Genivaldo Jualio Perpeatuob, Acta Cryst. (2008). C64, o91-o94.

24. W. Martanto, S. P. Davis, N. R. Holiday, J. Wang, H. S. Gill. and M. R. Prausnitz. Pharmaceutical Research, 2004, 21, 6, 947-952.

25. R. M. Bhardwaj, I. Oswald and A. J. Florence, Acta Cryst. (2012). E68, o3377.

26. H. B. Szczesniak, V. Patroniak, W. Radecka-Paryzek and M. Kubicki, Acta Cryst. (2009). C65, o371-o373.

27. M. A. Spackman. and D. Jayatilaka. Hirshfeld surface analysis, Cryst Engg. Comm. 2009, 11, 19-32.

28. J. J. McKinnon, D. Jayatilaka. and M. A. Spackman. Chem Comm, 2007, 3814–3816.

29. H. F. Clausen, M. S. Chevallier, M. A. Spackman. and B. B. Iversen. New J. Chem., 2010, 34, 193–199.

30. M. A. Spackman. and J. J. McKinnon. Cryst Engg. Comm. 2002, 4(66), 378–392.

31. S.K. Wolf, D.J. Grimwood, J.J. McKinnon, M.J. Turner, D. Jayatilaka, M. A. Spackmann. Crystal Explorer, University of Western Australia, Australia, 2009.

32. M.J. Frisch, G.W. Trucks, H.B. Schlegel, G.E. Scuseria, M.A. Robb, J.R. Cheeseman, G. Scalmani, V. Barone, B. Mennucci, G.A. Petersson, H. Nakatsuji, M. Caricato, X. Li, H.P. Hratchian, A.F. Izmaylov, J. Bloino, G. Zheng, J.L. Sonnenberg, M. Hada, M. Ehara, K. Toyota, R. Fukuda, J. Hasegawa, M. Ishida, T. Nakajima, Y. Honda, O. Kitao, H. Nakai, T. Vreven, J.A. Montgomery, Jr., J.E. Peralta, F. Ogliaro, M. Bearpark, J.J. Heyd, E. Brothers, K.N. Kudin, V.N. Staroverov, R. Kobayashi, J. Normand, K. Raghavachari, A. Rendell, J.C. Burant, S.S. Iyengar, J. Tomasi, M. Cossi, N. Rega, J.M. Millam, M. Klene, J.E. Knox, J.B. Cross, V. Bakken, C. Adamo, J. Jaramillo, R. Gomperts, R.E. Stratmann, O. Yazyev, A.J. Austin, R. Cammi, C. Pomelli, J.W. Ochterski, R.L. Martin, K. Morokuma, V.G. Zakrzewski, G.A. Voth, P. Salvador, J.J. Dannenberg, S. Dapprich, A.D. Daniels, O. Farkas, J.B. Foresman, J.V. Ortiz, J. Cioslowski, D.J. Fox, Gaussian-09, Revision D.01, Gaussian Inc, Wallingford, CT, 2009.

33. A.D. Becke, J. Chem. Phys. 98 (1993) 5648.

34. C. Lee, W. Yang, R.G. Parr, Phys. Rev. B 37 (1988) 785.

35. A.J. Rybarczyk-Pirek, L. Chęcińska, M. Małecka. and S. Wojtulewski. Cryst. Growth Des., 2013, 13, 3913–3924.

Figures

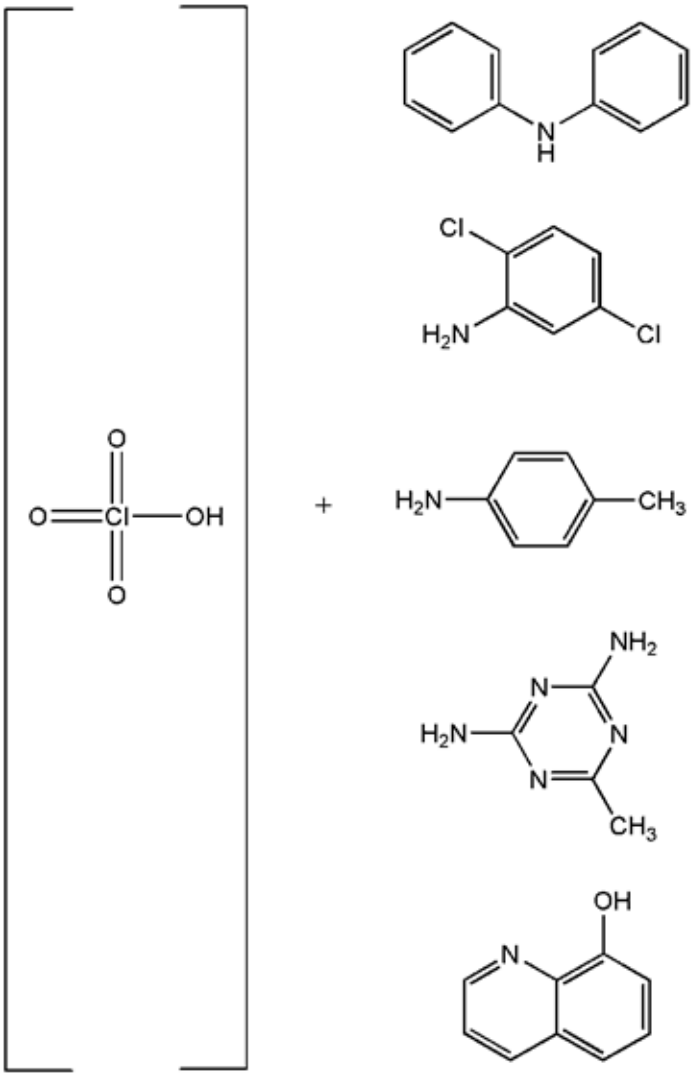

Figure 1

Figure 1

Chemical scheme of five perchlorate salts.

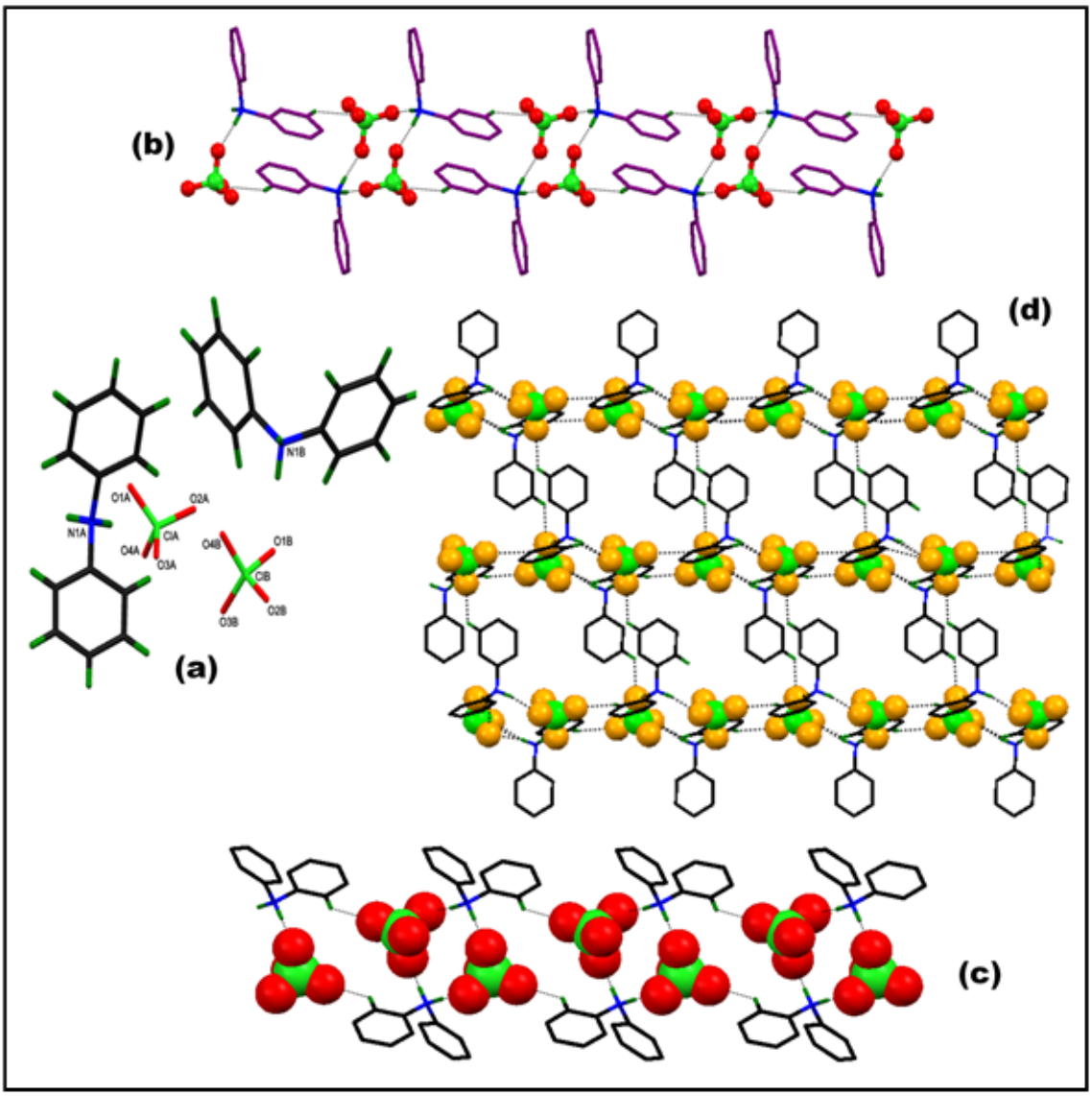

Figure 2

Figure 2

(a) The structure of 1, with labeling of atoms in the asymmetric unit (b) and (c) 1D Molecular Ladder of compound 1 (Molecule A and B) extended by hydrogen bonding interactions (d) 2D supramolecular network extended by C–H…O interactions. Perchlorate anions are displayed in space-filled model. (The hydrogen atoms not involved in the hydrogen bonding were removed for clarity)

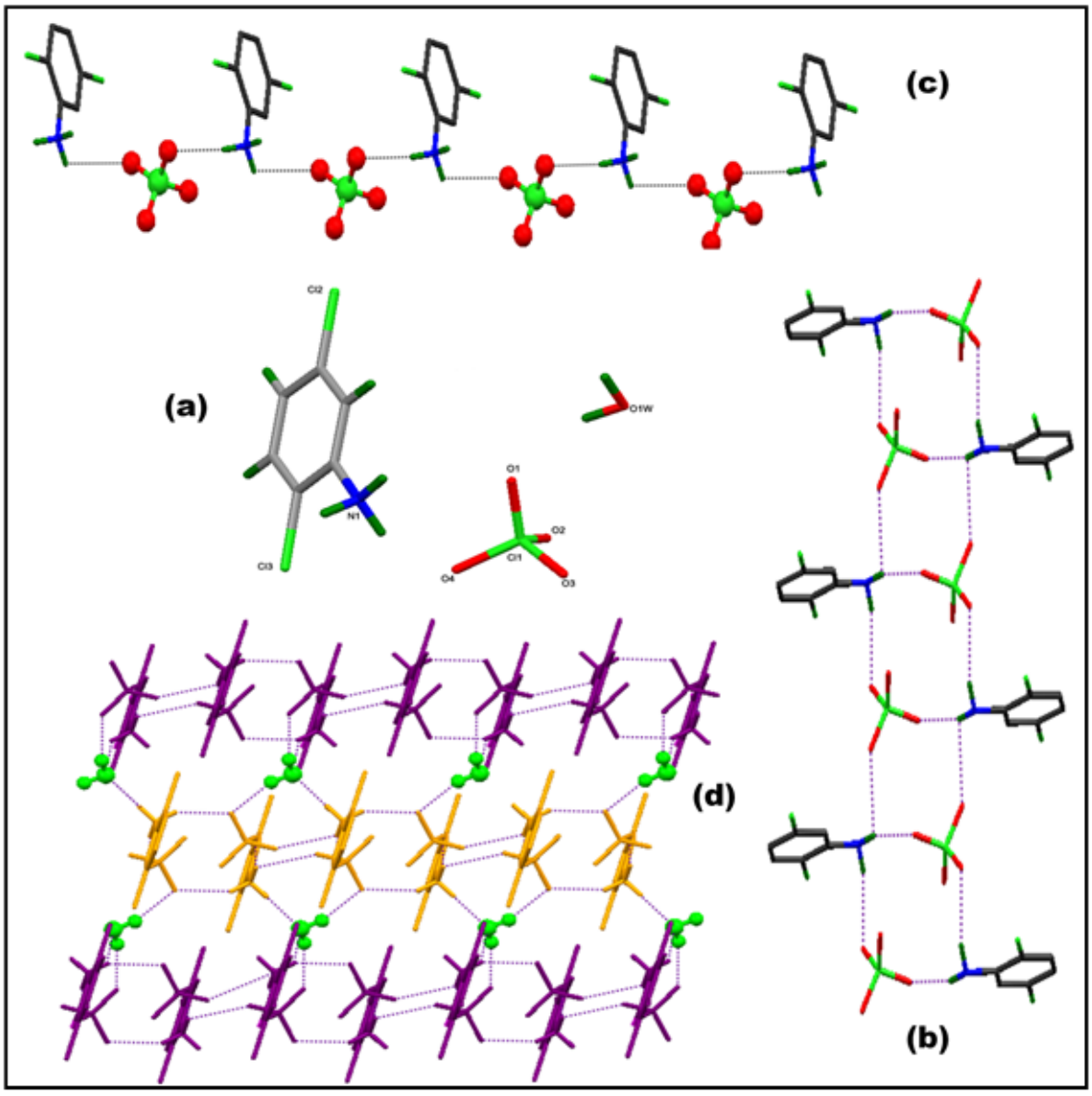

Figure 3

Figure 3

(a) Molecular structure of compound 2 with atom label of asymmetric unit (b) 1D supramolecular chain are connected by strong N-H..O hydrogen bond (c) 1D molecular ladder (d) 2D supramolecular network extended by water molecules through O-H…O interactions. The ball and stick representation of water molecules are highlighted in green color. (The hydrogen atoms not involved in the hydrogen bonding were removed for clarity)

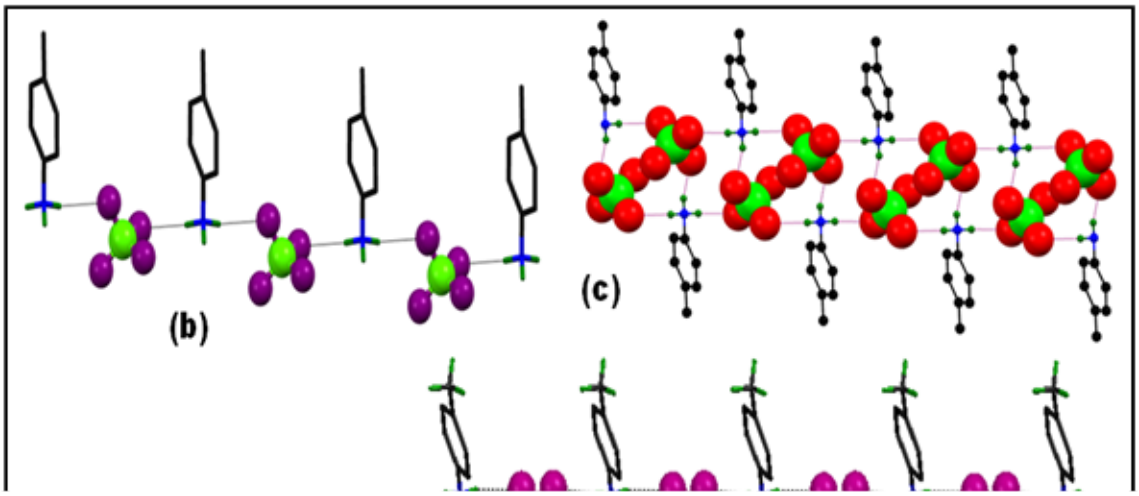

Figure 4

(a) Molecular structure of compound 3 with atom label of asymmetric unit (b) 1D anionic-cationic chain formed through N-H…O hydrogen bonds (c)1D molecular ladder (d) 2D molecular ladders are joined by hydrogen bonds. The perchlorate anions are indicated as different colors (purple, green and orange) in each ladder. (The hydrogen atoms not involved in the hydrogen bonding were removed for clarity)

Figure 5

(a) Molecular structure of compound 4 with atom label of asymmetric unit (b) 1D molecular ladder (c) Perchlorate anions are denoted as space-filling model to show the anion-cation interactions. (The hydrogen atoms not involved in the hydrogen bonding were removed for clarity)

Figure 6

(a) Molecular structure of compound 5 with atom label of asymmetric unit (b) 1D helical chain (c) 2D chain. (The hydrogen atoms not involved in the hydrogen bonding were removed for clarity)

Figure 7

Variety of supramolecular synthons present in perchlorate salts 1-5.

Figure 8

(a) Hirshfeld surfaces of the compound 1 (b) 2D finger plots derived from HS’s and (c) percentage contribution of all interactions around the cation-anion.

Figure 9

(a) Hirshfeld surfaces of the compound 2 (The surface was not kept transparent because the molecule inside the surface not look clearly in this orientation) (b) 2D finger print plot and (c) relative contribution of the whole interaction present.

Figure 10

(a) Hirshfeld surfaces of the compound 3 (b) two-dimensional finger plots sand (c) percentage contribution of all interactions over the compound.

Figure 11

(a) Molecular Hirshfeld surfaces of the compound 4 (b) associated 2D finger print plot and (c) relative contribution of the various interactions invovled.

Figure 12

(a) Hirsfield surface analysis of the molecule 5 (b) 2D fingerprint plot and (c) percentage contribution of the whole interactions associated in the molecule.

Figure 13

Molecular Electrostatic potentials mapping for (a) DPAPC, (b) 25DAP, (c) 4MAPC, (d) 24DAMTHP and (e) 8HQP.

Figure 14

the optimized molecular structures of the compounds 1-5. The discrepancies found may be change in phase of the system where the experimental structure belongs to crystalline state where intermolecular interactions play a major role while the predicted geometry is at gas state. No constraints and restraints were involved the molecules were allowed free to optimize.

Supplementary Files

This is a list of supplementary files associated with this preprint. Click to download.

- graphicalabstarct.doc